ACS OMEGA

http://pubs.acs.org/journal/acsodf

Article

Green and Scalable Preparation of Colloidal Suspension of Lignin Nanoparticles and Its Application in Eco-friendly Sunscreen Formulations

Davide Piccinino, Eliana Capecchi, Ines Delfino, Marcello Crucianelli, Nicola Conte, Daniele Avitabile, and Raffaele Saladino*

Cite This: *ACS Omega* 2021, 6, 21444−21456

Read Online

ACCESS | Metrics & More | Article Recommendations | Supporting Information

ABSTRACT: Lignin nanoparticles (LNPs) are applied in several industrial applications. The nanoprecipitation of LNPs is fast and inexpensive but currently still limited to the use of hazardous organic solvents, making it difficult to apply them on a large scale. Here, we report a scalable nanoprecipitation procedure for the preparation of colloidal lignin nanoparticles (cLNPs) by the use of the green solvents dimethylisosorbide and isopropylidene glycerol. Irrespective of the experimental conditions, cLNPs showed higher UV absorbing properties and radical scavenging activity than parent LNPs and raw lignin. cLNPs were successively used in the preparation of eco-friendly sunscreen formulations (SPF 15, 30, and 50+, as evaluated by the COLIPA assay), which showed high UV-shielding activity even in the absence of synthetic boosters (microplastics) and physical filters (TiO_2 and ZnO). Biological assays on human HaCaT keratinocytes and human skin equivalents demonstrated the absence of cytotoxicity and genotoxicity, associated with an optimal protection of the skin from UV-A damage.

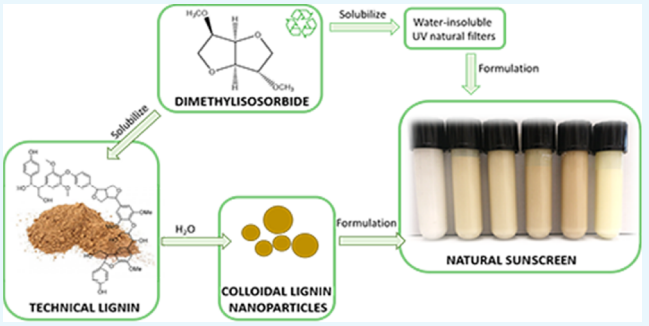

INTRODUCTION

The focus on renewable resources is increasingly growing, and the choice to remove petrochemical derivatives from commercial products is consolidated over time. In the last years, lignin, the most abundant polyphenol in nature, has received great attention due to its benign chemical and physical properties and green application in different fields,[1] including chelation[2] and in flame retardant,[3] metal adsorbent,[4] emulsifier, and cosmetic filler[5] applications. The absence of cytotoxicity associated with the antioxidant,[6] UV absorption,[7] and antimicrobial[8] properties makes lignin a suitable candidate in the formulation of cosmeceutical and pharmaceutical products.[9] Lignin remains a material not yet valued in the world market, with 98−99% being incinerated to produce energy. Only the remaining 1−2% is used for the production of lignosulfonates.[10] In addition, lignin nanoparticles (LNPs) produced by the nanoprecipitation technology[11] improve the radical scavenging and UV absorbing properties[12] of the polymer due to the emergence of hydrophobic and $\pi-\pi$ stacking interactions between the aromatic subunits.[13,14] LNPs are effective biocatalytic platforms[15] in biosensing[16] and bioink formulations.[17] The role of LNPs as UV filters in sunscreen formulations is well documented, and their sun protection factor (SPF) booster activity is carefully analyzed.[18,19] SPF boosters are common fillers used in commercial sunscreens to increase the total performance of UV filters by synergistic effects. Actually, these additives are mainly composed of oil-based polymers (e.g., microspheres of styrene/acrylate copolymers).[20]

During the nanoprecipitation process, lignin achieves an ordered spherical structure by the fast change in polarity between two miscible solvents.[21] The beneficial effect of organic solvent−water binary mixtures in favoring the solvation of both hydrophobic and hydrophilic groups of lignin has been reported, and their role in avoiding uncontrolled aggregation processes is discussed in detail.[22] The primary solvent is selected on the basis of its ability to solubilize lignin and for the recyclability and environmental impact, while the secondary solvent is water. The primary solvent are usually toxic and flammable organic derivatives, such as tetrahydrofuran (THF),[23] 1,4-dioxane,[24] acetone,[25] and dimethyl sulfoxide (DMSO),[26] showing low compatibility with large-scale industrial processes. Recent developments toward sustainable methods[27] including novel greener

Received: April 30, 2021
Accepted: July 16, 2021
Published: August 9, 2021

alternatives such as ethanol,[28] γ-valerolactone (GVL),[29] *p*-toluenesulfonic acid,[30] and deep eutectic solvents[31] were reported in a greener LNP nanoprecipitation procedure, focusing on the chemophysical properties of particles. The use of a green solvent allows expansion of the fields of application of LNPs, including nanomedicine, agrochemistry,[32] and food packaging.[33] Usually, the primary solvent is removed from the final solution to yield isolated LNPs by centrifugation and dialysis procedures. Otherwise, the colloidal lignin nanoparticles (cLNPs) can be obtained, maintaining the primary solvent. The latter case is of particular interest for the cosmetic industry, since it facilitates the direct preparation of formulations without the energy and time-demanding isolation of LNPs. The Food and Drug Administration and European Chemicals Agency highlighted the necessity to remove some of the actual commercial active principles and additives from sunscreen formulations due to their side effects on health and the environment.[34] For this reason, innovative and sustainable bio-based materials are required. To evaluate a larger panel of green solvents, we describe here the use of eco-certified dimethylisosorbide (DMI) and isopropylidene glycerol (IPG) in the nanoprecipitation of cLNPs from organosolv lignin (OL), kraft lignin (KL), and alkaline lignin (AL). The green and eco-friendly properties have been certified by the European Cosmetic Organic and Natural Standard (COSMOS) protocol globally recognized by the cosmetic industry and further validated by EHS standards.[35] Irrespective of the experimental conditions, the UV absorbing properties and radical scavenging activity of cLNPs were higher than those of corresponding LNPs and raw lignin. Four eco-friendly sunscreen formulations with different SPF values (15, 30, and 50+, in accordance with the European Cosmetic and Perfumery Association COLIPA classification) were prepared with KL-cLNPs using DMI. Furthermore, thanks to its high solvent capacity, DMI dissolved water-insoluble UV filters, avoiding the use of microplastic boosters and chemical and physical UV filters (TiO_2 and ZnO). Biological assay on HaCaT keratinocytes and human skin equivalents (HSEs) showed the absence of cytotoxicity and genotoxicity of the novel cLNPs and sunscreen formulations in association with the optimal protection of skin from UV-A damage.

RESULTS AND DISCUSSION

Procedure for the Preparation of Colloidal LNPs. Colloidal lignin nanoparticles (cLNPs) were prepared by the nanoprecipitation technique starting from commercially available OL, KL, and AL. The original composition of the starting lignin was determined by phosphorus nuclear magnetic resonance ^{31}P NMR analysis, as reported in Figure S1. Nontoxic, biodegradable, and eco-certified DMI and IPG were used as primary solvents,[36,37] and their effectiveness in the process was compared with GVL and THF. Table 1 reports the main chemophysical properties of selected solvents, and GVL was the only member of the series showing a partial miscibility with water. The solubility of OL, KL, and AL in the different solvents is reported in Table 2.

The lignin sample (0.3 g) was dissolved in an appropriate solvent (50 mL) by ultrasonication for 30 min at 50 °C. Then, deionized water (100 mL) was added in the frame of 1−2 s at 25 °C under mechanical stirring to obtain LNPs.[41] LNPs formed rapidly as a stable colloidal suspension (OL-cLNPs, KL-cLNPs, and AL-cLNPs). The total yield of the process, defined as milligrams of particles per milligram of the starting material (Table 2), was measured after the isolation of LNPs from the colloidal suspension. Irrespective of the original lignin, the highest yield was obtained with DMI (Table 2).

Table 1. Chemophysical Properties of Primary Organic Solvents Selected for the Nanoprecipitation of Lignin[a]

	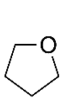 THF	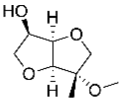 DMI	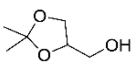 IPG	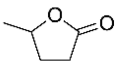 GVL
PM (g/mol)	72.11	174.19	132.15	100.12
d (g/L)	0.889	1.150	1.063	1.046
bp (°C)	66	236	188	207
H_2O misc.	total	total	total	100 mg/ml
Dielectric constant (ε)	7.6	6	Not available	36.5

[a]Data were obtained from refs 38−40.

Table 2. Solubility of the Starting Lignin in the Selected Solvents and Yield of LNPs

solvent	lignin	solubility (mg/10 mL)	yield (%)[a]
THF	OL	92.3 (28.0[b])	82.9
	KL	93.2 (9.0[b])	87.1
	AL	92.1 (55.0[b])	85.2
DMI	OL	92.0	87.7
	KL	96.1	91.1
	AL	94.0	89.2
IPG	OL	81.2	80.8
	KL	85.1	86.2
	AL	81.1	84.1
GVL	OL	88.2	85.9
	KL	90.6	89.6
	AL	89.1	89.1

[a]Yield was measured after the isolation of LNPs from the corresponding colloidal suspension. [b]Solubility data for EtOH.[42]

Field Emission Scanning Electron Microscopy, Dynamic Light Scattering, and ζ Potential Analyses. cLNPs were characterized by field emission scanning electron microscopy (SEM), dynamic light scattering (DLS), and ζ potential analyses, in comparison with colloidal particles from GVL and THF. Figure 1 reports the SEM images of cLNPs (upper panel) and the corresponding DLS analyses (lower panel). The grid connects different types of lignin with different primary solvents. cLNPs obtained from DMI showed a regular spherical shape similar to that obtained from GVL.

In contrast, IPG produced particles with irregular shape. Hydrodynamic diameter values, polydispersity index (PDI), and ζ potential of cLNPs are listed in Table 3. The hydrodynamic diameters of AL-cLNPs and KL-cLNPs obtained from DMI were smaller than those obtained from GVL and THF, with the nanoparticles produced from IPG showing the highest value. In addition, OL-cLNPs obtained from THF and GVL were smaller than that obtained from DMI, probably due to the higher hydrophobicity of OL with respect to AL and KL. Similarly, the PDI value of particles produced in DMI was always smaller than those of the other samples. KL-cLNPs, OL-cLNPs, and AL-cLNPs showed negative ζ potential values (Table 3), confirming the anionic character of the surface of the particles. The ζ potential of cLNPs was generally independent of the organic solvent used

https://doi.org/10.1021/acsomega.1c02268
ACS Omega 2021, 6, 21444−21456

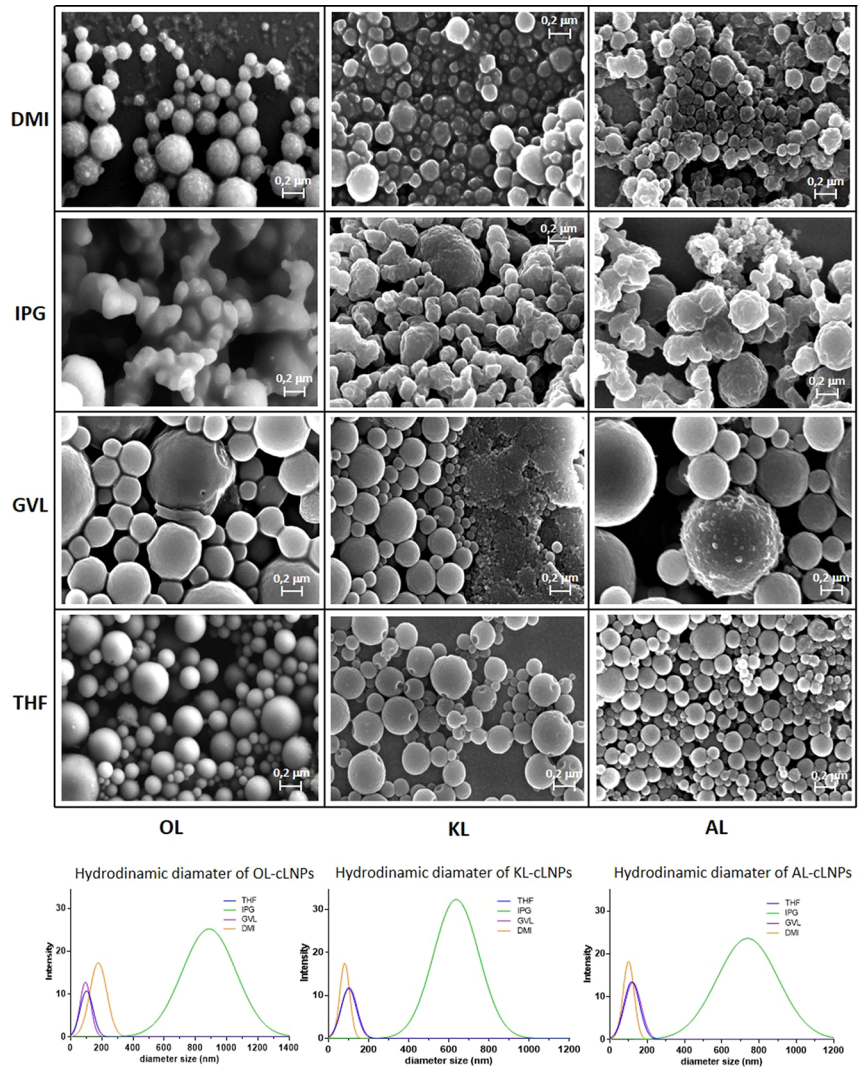

Figure 1. SEM images (upper panel) and DLS diagrams (lower panel) of KL-cLNPs, OL-cLNPs, and AL-cLNPs. The SEM image shows that the grid allows the connection of different types of lignin with different types of primary solvents used in the nanoprecipitation process.

Table 3. Mean Size, PDI, and ζ Potential Values of cLNPs Obtained from Different Primary Solvents

solvent	lignin	mean size (nm)	PDI[a]	ζ potential (mV)
THF	OL	99 ± 4.2	0.341	−32.2 ± 1.8
	KL	112 ± 5.1	0.232	−31.1 ± 1.9
	AL	118 ± 5.9	0.221	−29.9 ± 1.7
DMI	OL	192 ± 6.8	0.233	−33.4 ± 2.1
	KL	89 ± 3.9	0.101	−29.9 ± 0.8
	AL	102 ± 4.5	0.119	−32.5 ± 1.1
IPG	OL	905 ± 44.9	0.414	−27.3 ± 6.1
	KL	679 ± 33.5	0.471	−29.4 ± 4.8
	AL	780 ± 38.4	0.434	−28.6 ± 5.1
GVL	OL	101 ± 4.9	0.212	−31.4 ± 1.5
	KL	116 ± 5.2	0.232	−31.8 ± 1.1
	AL	121 ± 5.1	0.199	−32.8 ± 1.9

[a]PDI, polydispersity index.

in the nanoprecipitation process. These ζ potential values were probably responsible for repulsive interactions, avoiding particle aggregation.

Attenuated Total Reflectance Fourier Transform Infrared Analysis and ^{31}P NMR Characterization of LNPs. Isolated LNPs were characterized by attenuated total reflectance Fourier transform infrared analysis (ATR FT-IR; Figure 2). As a general trend, the main vibrational modes for lignin were not modified after nanoprecipitation, confirming the structural preservation of the native polymer. The C−H bending of methyl and methylene groups (1460 cm^{-1}) and the C═O (1600 cm^{-1}), C—H (2929 cm^{-1}), and O—H stretching (3433 cm^{-1}) were the most intense vibrational modes besides the fingerprint zone. LNPs obtained from DMI and GVL were also characterized by standard ^{31}P NMR spectroscopy and compared with parent lignin. The sample was solubilized in pyridine/$CDCl_3$ (300 µL; 1.6/1.0 v/v) under sonication conditions followed by quantitative derivatization with 2-chloro-4,4,5,5-tetramethyl-1,3,2-dioxaphospholane. Table 4 reports the functional group distribution of different types of OH moieties in LNPs.

The total amount of aromatic OH moieties was retained in both OL and KL nanoparticles from THF, DMI, and GVL, with the only exception of IPG, in which case the total content was lower than that of the reference. A different behavior was observed for AL nanoparticles characterized by a lower total amount of OH with respect to the original sample. In addition, the total amount of aliphatic OH groups was generally

https://doi.org/10.1021/acsomega.1c02268
ACS Omega 2021, 6, 21444−21456

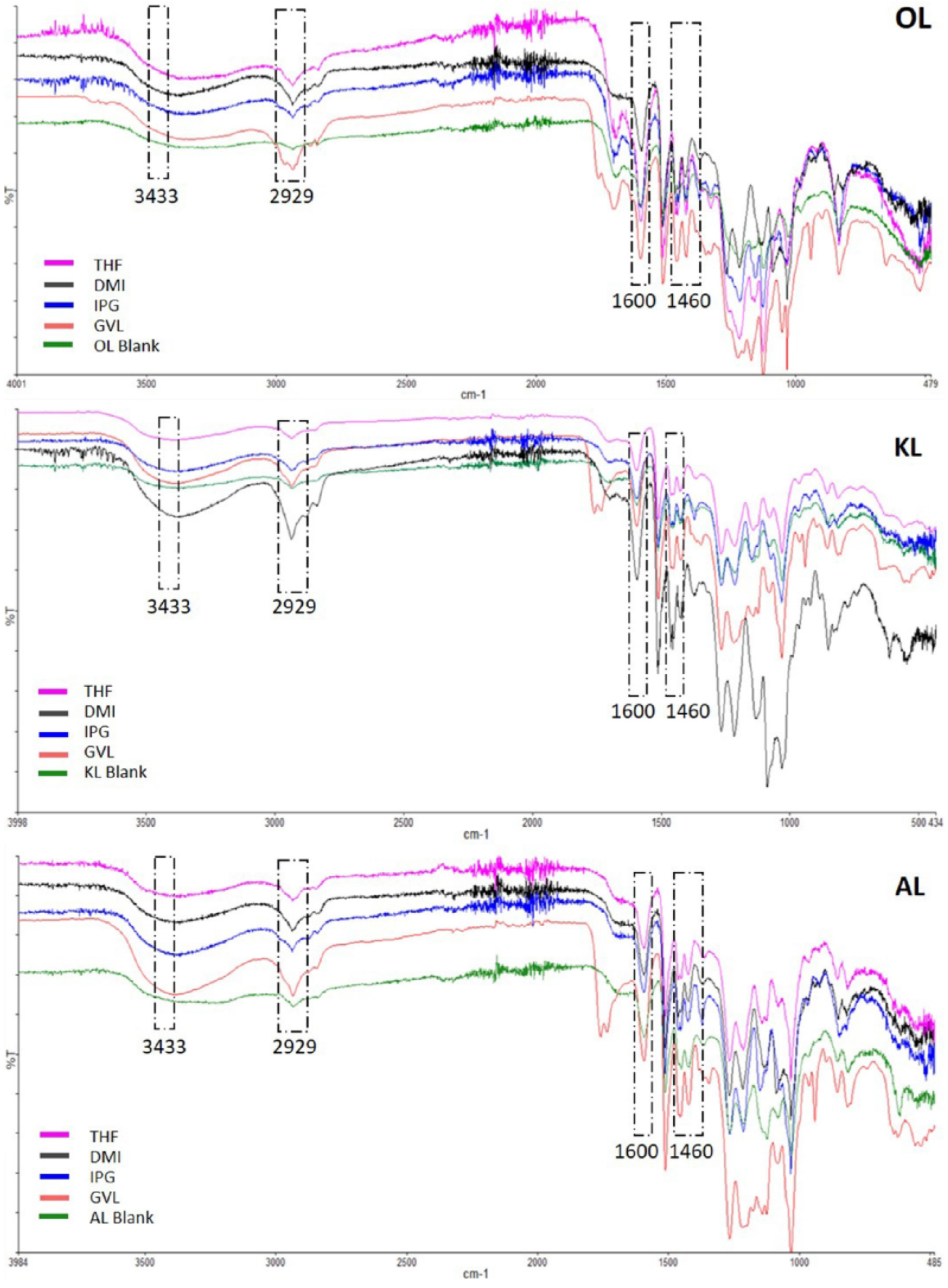

Figure 2. ATR FT-IR spectra of OL-LNPs, KL-LNPs, and AL-LNPs produced from different primary solvents. The analysis has been performed after the isolation of the particles. The spectra of native lignin are included as a reference.

retained. These results, taken together, confirmed that the average composition of native lignin was generally maintained in nanoparticles.

UV Absorption and Antioxidant Activity. The UV absorption capacity was evaluated for both LNP and cLNP samples. LNPs and cLNPs (0.05 mg/mL) were studied in the range of 190−700 nm at 25 °C (the absorption capacity of water and primary organic solvents was subtracted automatically during the analysis). As reported in Figure 3, LNPs from different origins showed a similar UV-B and UV-A absorbance

https://doi.org/10.1021/acsomega.1c02268
ACS Omega 2021, 6, 21444−21456

Table 4. Functional Group Distribution as Derived by Quantitative ^{31}P NMR Analyses of the Samples

sample		—COOH	aliphatic —OH	aromatic —OH[a,b]			
				S	G	H	ToT
	OL	0.97	2.28	1.09	1.21	0.15	2.45
	KL	0.21	1.62	0.01	1.62	0.02	1.65
	AL	0.20	1.59	0.02	1.51	0.03	1.56
THF	OL-LNPs	0.45	2.31	1.08	1.19	0.14	2.41
	KL-LNPs	0.20	1.63	0.00	1.65	0.01	1.66
	AL-LNPs	0.19	1.58	0.01	1.50	0.02	1.53
DMI	OL-LNPs	0.47	2.31	1.06	1.18	0.16	2.40
	KL-LNPs	0.23	1.69	0.00	1.59	0.01	1.60
	AL-LNPs	0.21	1.61	0.00	1.49	0.03	1.52
IPG	OL-LNPs	0.40	2.21	1.09	1.19	0.12	2.40
	KL-LNPs	0.16	1.49	0.01	1.41	0.01	1.43
	AL-LNPs	0.14	1.41	0.00	1.49	0.03	1.52
GVL	OL-LNPs	0.43	2.30	1.08	1.18	0.15	2.41
	KL-LNPs	0.22	1.64	0.00	1.59	0.02	1.61
	AL-LNPs	0.21	1.60	0.01	1.47	0.01	1.49

[a]S, syringyl units; G, guaiacyl units; and H, para-hydroxy phenolic units. [b]Millimoles/gram of unit.

capacity, always higher than that of the reference. UV absorbance of LNPs and cLNPs from THF is also reported as a reference. Notably, cLNPs were more efficient absorbers than the corresponding LNPs. This result was probably due to the effect of the colloidal aggregation state on the UV absorbance capacity.[43]

The following order of UV absorption capacity was observed for cLNPs: DMI > GVL > IPG. DLS analysis showed that KL-cLNPs were characterized by the lowest diameter value. This data can explain the higher UV-shielding capacity of KL-cLNPs with respect to the other lignin particles, since the distribution of chromophores and auxochromes between the surface and core of LNPs has been reported to depend on the particle size.[44]

The antioxidant activities of LNPs and cLNPs were evaluated by measuring the radical scavenging properties of the sample against 2,2′-diphenyl picrylhydrazyl radical (DPPH, 0.25 mM EtOH solution) at different concentration values (from 0.025 to 0.5 mg/mL) in MilliQ water using parent lignin as the reference. Table 5 reports the IC_{50} values (mg/mL of sample that causes 50% loss of DPPH concentration) and the radical scavenging index (RSI) (corresponding to the reciprocal value of IC_{50}). No antioxidant activity was recorded in the cases of DMI, IPG, and GVL alone. Again, the antioxidant activities of LNPs and cLNPs were higher than that of native lignin. In addition, cLNPs were more active than the corresponding LNPs, with the only exception for cLNPs prepared from IPG, for which an inverse trend was observed. Irrespective of the primary solvent used, KL was the most efficient lignin in scavenging the DPPH radical, followed by AL and OL. Finally, LNPs and cLNPs from DMI were characterized by the highest radical scavenging activity. The increase in the UV absorbing properties and antioxidant activity in nanoscaled LNPs has been reported and related to the $\pi-\pi$ self-aggregation of the aromatic subunits favoring the electron-transfer process.[45,46] In this context, the bathochromic shift we observed in LNP and cLNP samples (Figure 3) strongly suggests the formation of the head-to-tail J-type motif as the optimal aggregate state for the enhancement of the UV absorbing capacity.[25,47]

Generally, the primary solvent used to dissolve lignin can affect the morphological and chemical properties[48] of the starting material due to its interference with the network of noncovalent bonding in the polymer.[49] The influence of different selected binary solvents on LNP sizes has been reported.[50] In addition, the binary solvent can control the formation of the J-aggregate with respect to the H-aggregate as well as the correct arrangement of hydrophilic groups on the surface of the LNPs, thus affecting the UV photoabsorption and antioxidant capacity.

Procedure for the Preparation of Sunscreen Formulations and Evaluation of the Stability of Formulations. KL-cLNPs obtained from DMI were selected to prepare four novel sunscreen formulations. The sunscreen formulations were prepared by mixing a standard oil phase (coco-caprylate, mono- and triglycerides from coconut, Eumulgin VL-75, and tocopherol) with small amounts of natural UV filters (γ-oryzanol (γ-o) and α-bisabolol (α-BL); samples KL1−KL4; Table 6) with a water phase (glycerin, D-panthenol, and Xanthan gum) containing KL-cLNPs (1.0% and 2.5%, respectively, of the original colloidal suspension (1.0 g/mL)) in the presence of small amounts of natural secondary metabolites such as ferulic acid (FA), quercetin (Q), and gentisic acid (GA). Amounts of KL-cLNPs higher than 2.5% were not studied since they resulted in too dark formulations. An additional amount of DMI (5.0% and 10.0%) was also added to obtain complete homogenization of the formulation. A similar procedure was applied with KL-cLNPs (1.0%, 2.5%, and 5.0 % from the original colloidal suspension (1.0 g/mL)) in the absence of natural UV filters, to yield formulations B1−B3 (Table 6). Finally, formulation B4 was used as a negative control, having no KL-cLNPs and UV filters (Table 6). A commercial SPF50+ formulation (COM50+) was used as a reference. Figure 4 reports the coloration of KL-cLNP in eco-sustainable solvents (panel A) and in sunscreen formulations KL1−KL4 (panel B).

The UV transmittance spectra of KL1−KL4 and B1−B4 samples are reported in Figure 5 (panels A and B, respectively). As a general trend, KL1−KL4 showed lower transmittance values as compared to B1−B4 in all the wavelengths studied. The SPF, critical wavelength C_λ (defined as the wavelength at which the integral of the spectral absorbance curve reaches 90% of the integral from 290 to 400 nm), and UV-A/UV-B ratio (UV ratio) values are listed in

https://doi.org/10.1021/acsomega.1c02268
ACS Omega 2021, 6, 21444−21456

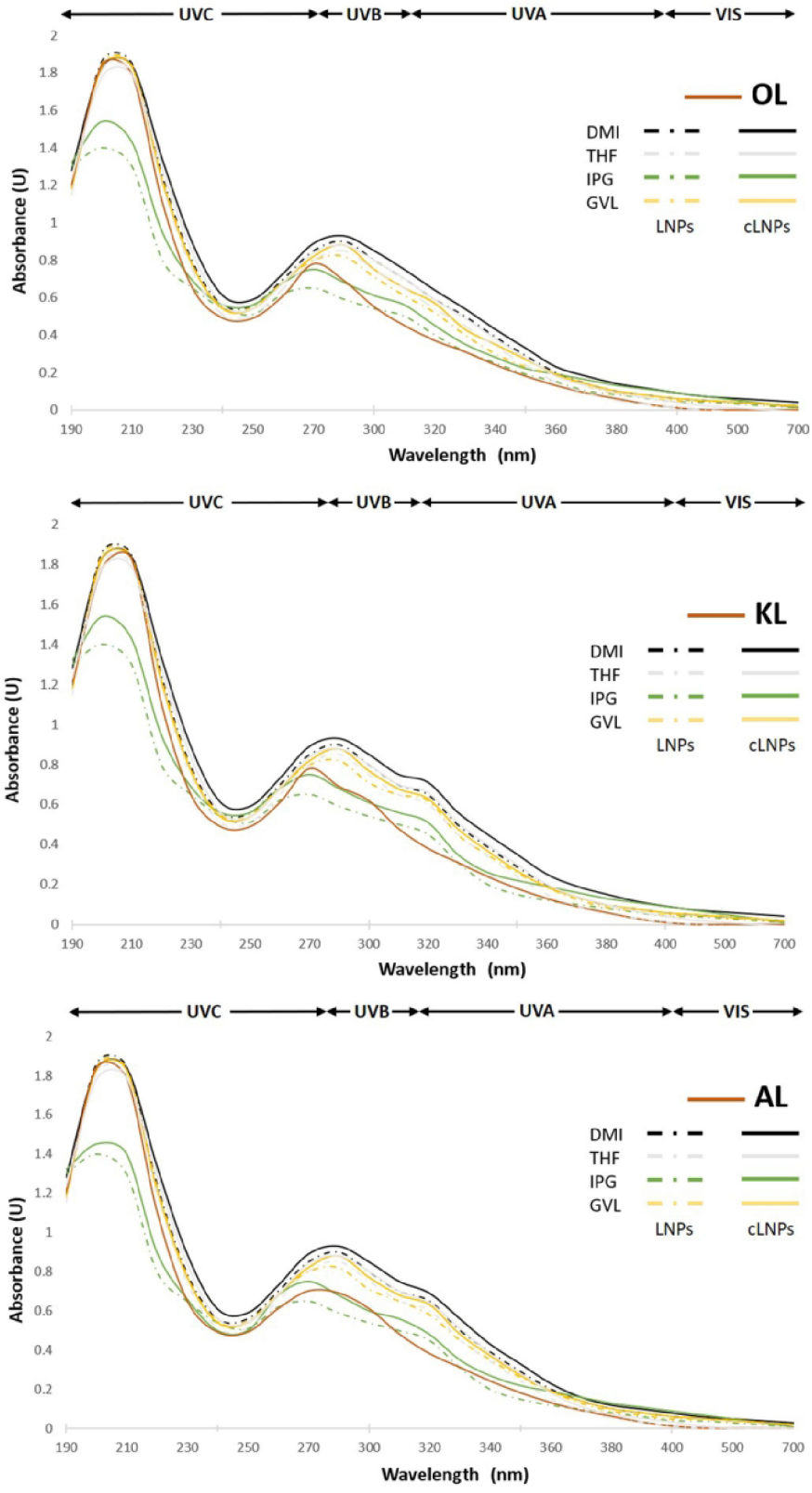

Figure 3. UV absorbance capacity of LNPs and cLNPs. The analysis was performed with the appropriate sample (0.05 mg/mL) in the range from 190 to 700 nm at 25 °C under gentle stirring. Native amorphous lignin was used as a reference. Both UV-B and UV-A ranges are reported.

Table 6 (data referring to samples KL1−KL4 characterized by the presence of other actives and the absence of KL-cLNPs are reported in parentheses). Among the B1−B3 formulations (without additional filters different from KL-cLNPs), the SPF values well correlated with the lignin content. Indeed, formulation B3 displayed the highest SPF value (2.91; Table 6). Better results were obtained by adding natural UV filters to formulations. In particular, formulations KL3 and KL4 showed

https://doi.org/10.1021/acsomega.1c02268
ACS Omega 2021, 6, 21444−21456

Table 5. Antioxidant Activity of LNPs

	sample	IC_{50}	RSI[a]	sample	IC_{50}	RSI[a]
	OL	0.035	28.57			
	KL	0.026	38.46			
	AL	0.031	32.26			
THF	OL-LNPs	0.027	37.03	OL-cLNPs	0.026	38.46
	KL-LNPs	0.022	45.45	KL-cLNPs	0.021	47.65
	AL-LNPs	0.024	41.66	AL-cLNPs	0.023	43.41
DMI	OL-LNPs	0.026	38.46	OL-cLNPs	0.021	47.62
	KL-LNPs	0.018	55.56	KL-cLNPs	0.014	71.44
	AL-LNPs	0.023	43.48	AL-cLNPs	0.018	55.61
IPG	OL-LNPs	0.031	32.26	OL-cLNPs	0.039	25.69
	KL-LNPs	0.022	45.45	KL-cLNPs	0.025	40.06
	AL-LNPs	0.026	38.46	AL-cLNPs	0.029	34.50
GVL	OL-LNPs	0.028	35.71	OL-cLNPs	0.027	37.03
	KL-LNPs	0.02	50.00	KL-cLNPs	0.019	52.69
	AL-LNPs	0.023	43.41	AL-cLNPs	0.021	47.65

[a]RSI parameter is defined as the reciprocal of IC_{50}.

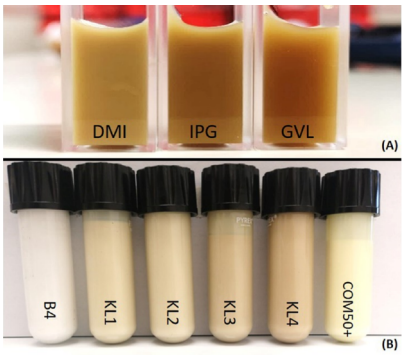

Figure 4. (A) Coloration of KL-cLNPs prepared in the three eco-sustainable organic solvents (DMI, IPG, and GVL). (B) Colorations of sunscreen formulations KL1−KL4 in relation to the amount of KL-cLNPs, B4, and COM50+ are reported as references.

the highest SPF (31.1 and 60.5, respectively), C_λ, and UV ratio values, of the same order of magnitude of the reference values established by the EU regulation (Regulation (EC) No. 1223/2009; C_λ > 370 nm; UV ratio > 0.33). In accordance with the data in Table 6, increased amounts of FA and GA, besides the higher concentration of α-BL, afforded better results. These results showed that KL-cLNPs at concentrations up to 5% do not act as UV filters such as the SPF booster ingredient. The SPF boosters are additives that weakly absorb UV rays but are able to increase the performance of UV filters by synergistic physical and transfer electron processes.[51] Indeed, in mixture with natural UV filters (FA, Q, and GA), KL-cLNPs displayed a synergy UV boosting effect (BE), starting from around 74.2% (Table 6). The BE increased dose dependently with the total amount of cLNPs, reaching its highest value (93.3%) in the case of sample KL4. Petrochemical derivatives are usually employed in commercial products (from 2.5% to 12% in weight), with a maximum reported BE of 20%.[21] Microplastics are very dangerous for the environment due to their toxicity and implications for human health.[52] Noteworthily, KL-cLNPs showed an overall BE higher than microplastics. In addition, the SPF value of KL4 was similar to that observed for the Com50+ formulation, despite the lower number of UV filters (20.8% vs 37.6%) and the absence of metal oxides such as titanium dioxide or hydroxyapatite. The stability of the most active samples KL3 and KL4 was evaluated by measuring the SPF, C_λ, and UV ratio values after treatment at 50 °C for 60 days under dark conditions. Under these experimental conditions, SPF values of 30.8 and 60.1 were obtained, respectively, confirming the retained stability of the formulations. Data on the BE of LNPs prepared from THF are

Table 6. SPF, C_λ Value, and the UV-B/UV-A Ratio (UV_{ratio}) of KL-cLNP-Based Sunscreen Formulations[a]

phase	UV filter[b]	B1	B2	B3	B4	KL1	KL2	KL3	KL4	COM50+
oil phase (4.0% coco-caprylate, 3.0% mono- and triglycerides from coconut, 2.8% Eumulgin VL-75, and 0.7% tocopherol)	γ-*o*					2.0%	5.0%	5.0%	5.0%	BEMT[b]
	α-BL					0.5%	0.5%	1.0%	1.0 %	TiO_2
water phase (3.0% glycerin, 0.5% D-panthenol, and 0.2% Xanthan gum)	FA					3.0%	5.0%	6.0%	8.0%	S2E
	KL-cLNPs	1.0%	2.5%	5.0%		1.0%	2.5%	2.5%	2.5%	SAC
	Q					0.3%	0.3%	0.3%	0.3%	DHHB
	GA					1.0%	1.0%	2.0%	4.0%	EMC
	DMI					1.0%	2.0%	2.0%	5.0%	HA
total filter (%)		1.0	2.0	5.0	0	7.8	14.3	16.8	20.8	37.6
SPF[c]		1.09	1.88	2.91	0.4	5.4 (3.1)	15.1 (8.3)	31.1 (16.4)	60.9 (31.5)	63.5
C_λ		290	348	358	290	365 (356)	369 (359)	370 (361)	371 (363)	373
UV_{ratio}		0.92	0.86	0.82	1.1	0.49 (0.59)	0.45 (0.56)	0.39 (0.48)	0.36 (0.46)	0.39
boosting effect (%)[d]						74.2	81.9	89.6	93.3	

[a]B1−B3: formulations containing different amounts of KL-cLNPs in the absence of UV natural filters. B4: formulation without KL-cLNPs and UV natural filters. KL1−KL4: formulations containing KL-cLNPs in the presence of UV natural filters. COM50+: commercially available sunscreen used as a reference. [b]Description of the acronyms used for the UV natural and synthetic filters: FA, ferulic acid; Q, quercetin; γ-*o*, γ-oryzanol; GA, gentisic acid; α-BL, α-bisabolol; BEMT, bis-ethylhexyloxyphenol methoxyphenyl triazine; EMC, ethylhexyl methoxycinnamate; S2E, 2-ethylhexyl salicylate; SAC, styrene/acrylate copolymer (synthetic booster); DHHB, diethylamino hydroxybenzoyl hexyl benzoate; and HA, hydroxyapatite. [c]SPF, sun protection factor; λ_{crit}, wavelength at which the integral of the spectral absorbance curve reaches 90% of the integral from 290 to 400 nm maximum value of transmittance; UV ratio, UV-B/UV-A. The values of these parameters recorded in the absence of KL-cLNPs are reported in parentheses. [d]The boosting effect was calculated following eq 1.

https://doi.org/10.1021/acsomega.1c02268
ACS Omega 2021, 6, 21444−21456

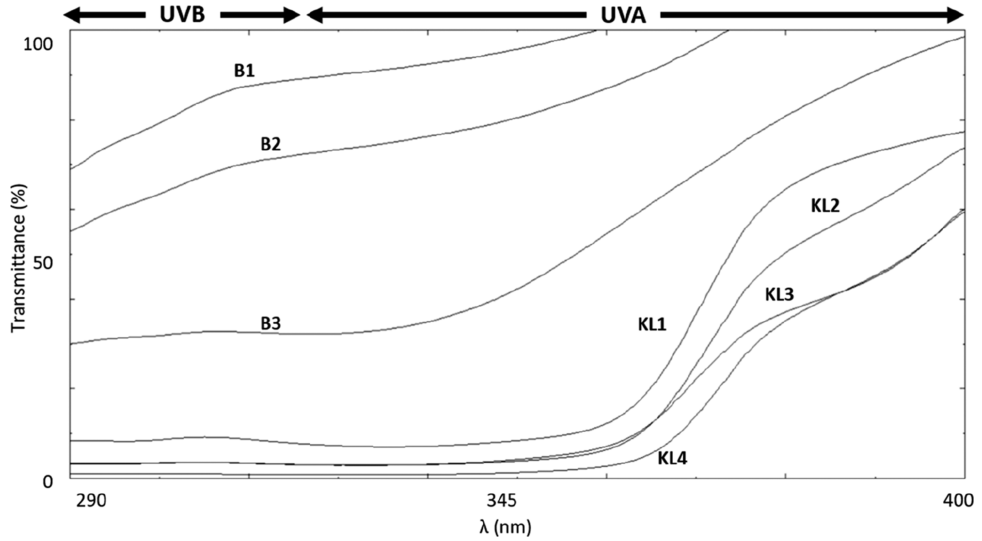

Figure 5. Transmittance of KL1−KL4 and B1−B3 sunscreen formulations prepared with KL-cLNPs. The composition of samples KL1−KL4 is reported in the text. Samples B1−B3 did not contain natural UV filters different from KL-cLNPs.

reported. This effect was of the same order of magnitude than that observed with LNPs from DMI.[20]

Biological Assay. *KL-LNPs Protect against UVA-Induced Cell Death.* The cytotoxicity of KL-LNPs was evaluated in the human keratinocyte cell line HaCaT. The absence of cytotoxicity for amorphous lignin[53] and KL-LNPs prepared from THF has been previously reported and discussed.[14] HaCaT keratinocytes were incubated for 24 h with different concentrations of KL-LNPs prepared from DMI (0, 0.1, 0.5, 1.0, 5.0, and 10.0 μg/mL; water suspension), and their viability was tested by the MTT assay. A solution of 1.0% sodium dodecyl sulfate in purified water (SDS 1.0%) was employed at the same range of concentration as a positive control. As expected, SDS (1.0%) increased cell toxicity dose dependently. Noteworthily, KL-LNPs showed no cytotoxicity at any of the assayed concentrations (n = 5; Figure 6, panel A). To evaluate the ability of KL-LNPs to protect against UVA-induced cell death, HaCaT cells were preincubated for 5 h with 0, 0.1, 0.5, or 1.0 μg/mL KL-LNPs and then irradiated with UV-A at the cytotoxic dose of 15 J/cm^2 for 5 min. UV-A treatment significantly reduced HaCaT cell viability in the absence of KL-LNPs. Importantly, KL-LNPs protected HaCaT cells dose dependently reaching their maximum activity at a concentration of 1.0 μg/mL (Figure 6, panel B).

KL-LNPs Protect against UVA-Induced Cell Death in Sunscreen Formulations. Cytotoxicity and UVA protection of KL-LNPs were successively evaluated in sunscreen formulations. Cytotoxicity was assayed for KL4 at different concentrations (0, 0.1, 0.5, and 10.0 μg/mL) and compared with data recorded in the absence of KL-cLNPs (KL4$^-$). Noteworthily, KL4 was not toxic at any of the tested concentrations (Figure 7, panel A).

The cytoprotective property of KL4 was assayed, as already described for KL-LNPs. HaCaT cells were preincubated with different concentrations of KL4 (0, 0.1, 0.5, and 1.0 μg/mL) for 5 h and then irradiated (or not) with 15 J/cm^2 UV-A for 5 min at room temperature and cultured for an additional 24 h under standard conditions. At the end of the incubation period, cell viability was assessed by the MTT assay. In the absence of the KL4 formulation, UV-A-treated HaCaT cells displayed a significant increase in cell death, as expected.

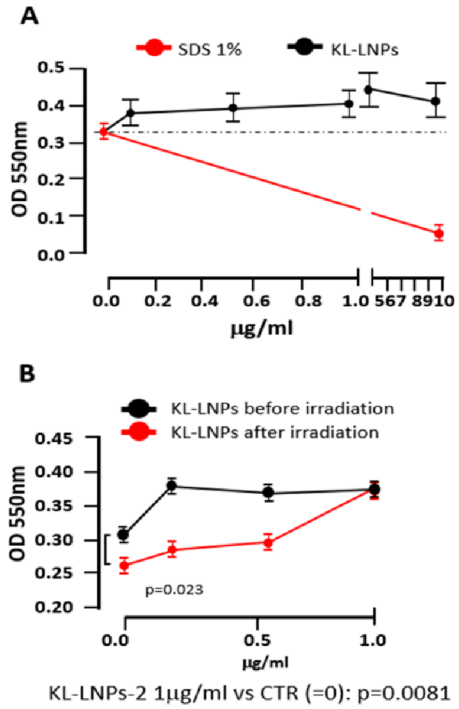

Figure 6. (A) Cytotoxicity of KL-LNPs prepared from DMI. The cell viability was expressed as the variation of the optical density (OD) value at 550 nm. (B) UV-A damage protection of KL-LNPs prepared from DMI. The cell damage was quantitatively assessed by the MTT assay.

Importantly, the viability of UV-A-treated cells was not significantly different from untreated cells in the presence of KL4. This result clearly demonstrates the safety and cytoprotective activity of KL4 (Figure 7, panel B). The cytoprotective assay of KL4 was also performed under more physiological conditions using an HSE model prepared starting from the human keratinocyte HaCaT cell line (details are provided in the Experimental Section).[54] HSEs were preincubated with samples for 5 h, irradiated with UV-A (15 J/cm^2) for 15 min, and incubated under standard culture conditions for an additional 18 h. Water (negative control,

https://doi.org/10.1021/acsomega.1c02268
ACS Omega 2021, 6, 21444−21456

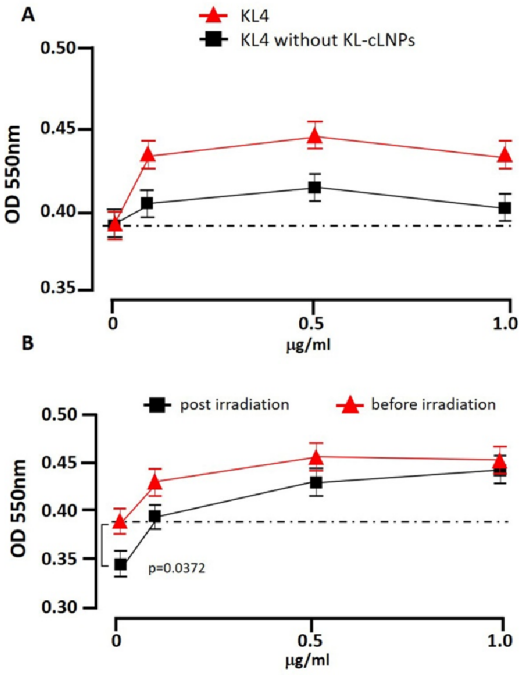

Figure 7. (A) Cytotoxicity of the KL4 sample. The cell viability was expressed as variation of the OD value at 550 nm. (B) UV-A damage protection of KL4 prepared from DMI. The cell damage was quantitatively assessed by the MTT assay.

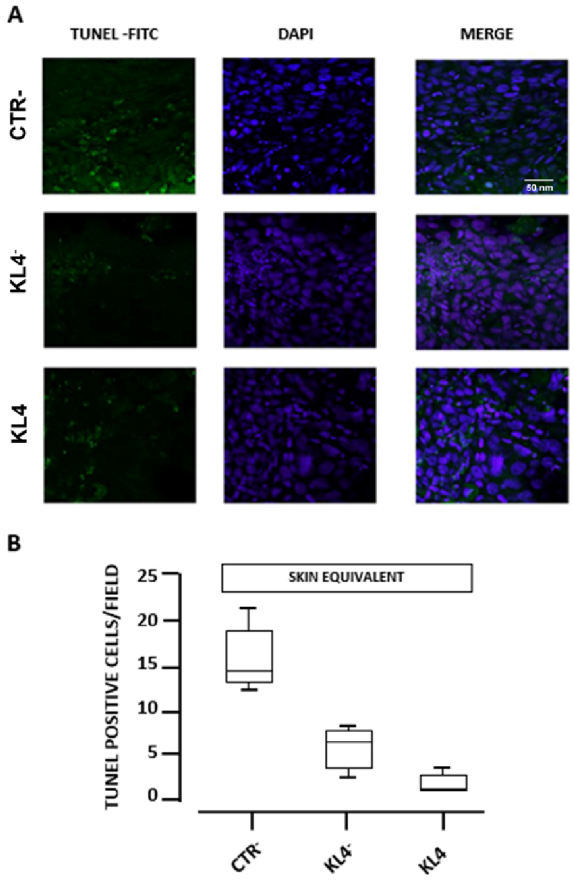

Figure 8. Evaluation of the genotoxicity of KL4 by the skin equivalent assay (HSE). (A) Images of histological analysis. (B) Quantitative analysis of the TUNEL positive cells. Statistical analysis was performed by the one-way ANOVA method followed by the Bonferroni test.

CTR$^-$) and KL4 without KL-cLNPs (KL4$^-$) were used as experimental references. At the end of the incubation period, HSEs were processed, and apoptosis was determined by a standard terminal 2′-deoxy-uridine nick and labeling assay (TUNEL assay). As expected, UV-A treatment induced a significant increase in apoptotic TUNEL$^+$ cells. Apoptotic cells were significantly reduced in the presence of both KL4 and KL4 without KL-LNP formulations. Moreover, the cytoprotective effect of KL4 was higher than the one observed for KL4 without KL-LNPs, demonstrating the efficacy of KL-LNPs (Figure 8).

CONCLUSIONS

Phototoxic and photoallergic responses associated with traditional UV filters have been reported,[55] as well as long-term photoaging and cell damage effects.[56] The use of biocompatible and eco-friendly ingredients completely devoid of toxic effects, such as lignin, can solve this problem, leading to safer formulations, with improved SPF values and eliminating dangerous booster additives such as microplastics. In this context, lignin has been selected during molecular evolutions to minimize the damage caused by UV radiation and chemical oxidative stress in the plant cell.[57] KL-cLNPs prepared by nanoprecipitation of KL from DMI showed the highest UV absorbing capacity and antioxidant activity compared to the corresponding cLNPs from GVL, IPG, and THF. In addition, KL-cLNPs suspended in DMI can be directly included in sunscreen formulations, thanks to the recognized eco-certification degree of DMI, while conventional solvents, such as THF, need to be removed before the application for regulatory concerns. As a general trend, KL-cLNPs performed better than OL-cLNPs and AL-cLNPs as an UV absorber and an antioxidant. KL-cLNPs from DMI were always characterized by their lowest hydrodynamic diameter and slightly lighter yellow color. KL-cLNPs were used for the preparation of four eco-friendly sunscreen formulations (KL1−KL4) in which the LNPs showed an UV BE significantly higher than that reported for microplastics. The KL4 formulation performed similarly to the commercial sample Com50+ characterized by a higher amount of synthetic UV filters. The novel formulations did not show cytotoxicity and genotoxicity effects on both HaCaT cells and HSEs. The BE of cLNPs and the absence of toxicity associated with high biocompatibility and biodegradability make KL-cLNPs an optimal green alternative for the preparation of environmentally friendly sunscreen formulations.[58]

Experimental Section. *Materials.* OL from hardwood (average M_w 3500 g mol^{-1}) was purchased from Chemical Point UG (Oberhaching, Germany). KL from softwood was purchased from Stora Enso (average M_w 6000−7000 g mol^{-1}). AL (average M_w 10,000 g mol^{-1}), 2-chloro-4,4,5,5-tetramethyl-1,3,2-dioxaphospholane (TMDP), chromium (III) acetylacetonate, *N*-hydroxy-5-norbornene-2,3-dicarboximide (NHND), DPPH, FA, Q, γ-o, α-BL, MTT (3,(4,5-dimethylthiazol-2)2,5 difeniltetrazolium bromide), SDS, and organic solvents were purchased from Sigma-Aldrich (St. Louis, MO, USA) and used without further purification. Commercial lignins were purified before use by standard procedures including alkali−acid treatment and continuous washing with deionized water. Ingredients for the emulsion (coco-caprylate, mono- and triglycerides from coconut, Eumulgin VL-75, α-tocopherol,

https://doi.org/10.1021/acsomega.1c02268
ACS Omega 2021, 6, 21444−21456

glycerin, D-panthenol, and Xanthan gum) were purchased from Sigma-Aldrich (St. Louis, MO, USA). DAPI and HaCaT were purchased from Thermo Fisher. The TUNEL-FITC assay kit was supplied by Roche Applied Science.

General Procedure to Prepare cLNPs and LNPs. Colloidal lignin nanoparticles were prepared by the nanoprecipitation method. The selected lignin was dissolved in an appropriate solvent (from 0.01 to ca. 0.3 g, 50 mL) until complete dissolution using an ultrasonication bath for 30 min at 50 °C or for 24 h under magnetic stirring at 25 °C. Successively, H_2O MilliQ (100 mL) was added under gentle stirring to yield the colloidal lignin nanoparticles (cLNPs). For the preparation of dry LNPs, the organic solvent was removed by dialysis using a 3.5 kDa SnakeSkin dialysis tube and the lyophilized crude.

Determination of Solubility and Yield of LNPs. The solubility of native lignin was calculated for each organic solvent and compared with THF. Generally, 100.0 mg of appropriate dried lignin was dissolved in 10 mL of select solvent by sonication for 30 min using a water bath sonicator at 50 °C. The lignin solution was centrifuged for 20 min at 11,000 rpm to recover the insoluble fraction, when present. The recovered insoluble part was dried and weighed. The solubility of lignin was calculated by subtracting the insoluble fraction from the initial weight. The final yield of LNPs, defined as milligrams of particles per milligram of the starting material, was calculated after the isolation through centrifugation of the particles from the colloidal suspension followed by lyophilization.

General Procedure for the Preparation of Sunscreen Formulations. KL-cLNP suspension was used after concentration by centrifugation and resuspension in the same binary system solvent (DMI/H_2O with 1:2 ratio), obtaining 1.0 g/mL suspension. The percentage amounts of ingredients were expressed in w/w. The sunscreen formulations were prepared by a direct emulsion procedure. The oil phase (10 g; 4.0% coco-caprylate, 3.0% mono- and triglycerides from coconut, 2.8% Eumulgin VL-75, and 0.7% tocopherol; all amounts are expressed as wt %) in the presence of the appropriate amounts of γ-o(2.0−5.0%) and α-BL (0.5−1.0%) was mixed with a water phase (90 g; 3.0% glycerin, 0.5% D-panthenol, 0.2% Xanthan gum, and H_2O MilliQ) containing KL-cLNPs [1.0% and 2.5% from the original colloidal suspension (1.0 g/mL)] and the appropriate amounts of FA (3.0−8.0%), Q (0.3%), and GA (1.0−4.0%). The homogeneity of the formulation was optimized by adding an additional amount of DMI (1.0−5.0%). A similar procedure was applied by using KL-cLNPs [1.0%, 2.5%, and 5.0% of the original colloidal suspension (1.0 g/mL)] in the absence of UV filters.

ATR FT-IR Analysis. ATR-IR analysis was performed at room temperature with a Perkin−Elmer "Spectrum One" spectrometer (Waltham, MA, USA) equipped with an ATR-IR cell. The IR spectra were recorded by averaging 32 scans with a resolution of 4 cm^{-1}.

^{31}P NMR Analysis. ^{31}P NMR analyses were acquired by a 400 MHz Bruker spectrometer (Billerica, MA, USA) with a 90° pulse width, 1.2 s acquisition time, and 25 s pulse delay to collect 64 scans. The appropriate lignin sample (10−20 mg) was phosphorylated with 60 μL of TMDP in 700 μL of pyridine/$CDCl_3$ (1.6:1, v/v) using chromium (III) acetylacetonate (1.0 mg/mL) as the relaxation agent and NHND (0.8 mmol) as the internal standard. The quantitative analysis was carried out using the Topspin 5.0 software.

Hydrodynamic Diameter and ζ Potential Analyses. Measurements of hydrodynamic diameter and ζ potential values were performed by resuspending freshly prepared cLNPs in H_2O by DLS using a Zetasizer Nano ZS (Malvern Instruments, Malvern, U.K.) apparatus, equipped with an He−Ne laser (633 nm, a fixed scattering angle of 173°, 25 °C). Measurements were performed in triplicate at room temperature (T = 25 °C).

SEM Analysis. SEM was carried out using ZEISS Gemini 500 (Oberkochen, Germany) at 5 kV. As a general procedure, LNPs in water dispersion (20 μL) were deposited on a coverslip coated with gold by sputtering (AGAR Automatic Sputter Coater) and dehydrated in air. The coverslip was mounted on the stub with conductive carbon glue, and a thin film (5.0 nm) of chromium was deposited onto the sample using the Sputter Quorum Q150T ES plus to make the sample enough conductive for measurement purposes.

Antioxidant Activity. The radical scavenging properties of LNPs and cLNPs were evaluated by the DPPH assay. Briefly, an appropriate amount of LNPs or cLNPs (0.001−0.5 mg mL^{-1} in MilliQ water), or alternative raw lignin (0.001−0.5 mg mL^{-1} in DMSO), was added to freshly prepared DPPH solution (0.25 mM in EtOH). The decrease in absorbance (517 nm) was detected using an UV−vis spectrophotometer (Varian Cary50 UV) at different time ranges and concentrations until the reaction reached a plateau. The kinetics of the radical scavenging process was studied for each concentration, and the amount of the residual DPPH was estimated. This value was used to calculate the IC_{50} (defined as the concentration of substrate in mg/mL that causes 50% loss of DPPH activity) and further expressed by the RSI value corresponding to the reciprocal value of IC_{50}.

UV Shielding Assay. The UV absorption property of cLNPs and LNPs (0.05 mg/mL) in a quartz cuvette (3.0 mL) was determined using a Varian Cary 50 UV scan (Crawley, U.K.) in the range from 190 to 700 nm at 25 °C under gentle stirring. The original cLNP suspension was diluted, maintaining the initial solvent ratios. The LNPs were resuspended in H_2O after purification from original solvents. The analysis was elaborated by the UV−vis scan software. The SPF value was calculated following the European COLIPA protocol[59] using a Shimadzu UV-2600 spectrophotometer (Kyoto, Japan) equipped with an integration sphere for the collection of the UV transmittance spectra of the sunscreen formulations. The sample was coated (1.3 mg/cm^2) on PMMA plates (5.0 cm^2 with a textured upper surface) followed by incubation in the dark at room temperature for 15 min and subsequently analyzed in the transmittance mode (the dose of UV delivered during one measurement cycle was 0.18 J/cm^2) using the UV Probe software. The spectrum obtained was finally converted by the SPF calculator software to extrapolate the final SPF value. The BE was expressed in percentage and calculated as follows:

$$\mathrm{BE} = \frac{\mathrm{SPF_f} - \mathrm{SPF_i}}{\mathrm{SPF_f}} \times 100 \quad (1)$$

where SPF_i = KL1−KL4 formulations in absence of KL-cLNPs and SPF_f = KL1−KL4 formulations

Cell Viability Assay. The cytotoxicity of KL-LNPs and KL4 samples was determined using the 3-(4,5-dimethylthiazol-2-yl)-2,5 diphenyltetrazolium bromide (MTT) test (reduction to the corresponding blue formazan) on the viability of HaCaT cells by spectrophotometric analysis at 550 nm. This biological

https://doi.org/10.1021/acsomega.1c02268
ACS Omega 2021, 6, 21444−21456

test involves culturing the cells for 24 h before and after treatment with the appropriate sample to be tested. SDS (1.0%, water solution) was used as a positive cytotoxicity control. The evaluation of cytotoxicity was performed using a concentration-dependent curve carried out starting from the concentration of 0.1 up to 10 μg/mL. The measurements were repeated five times. To evaluate the cell viability after UV-A exposition, HaCaT cultures were exposed to radiation before and after the treatment with KL-LNPs or KL4. Briefly, HaCaT cells were treated with the appropriate amount of the samples (0.1, 0.5, and 1.0 μg/mL), and after 5.0 h, they were exposed at an UV-A cytotoxic dose (15 J/cm^2) for 5 min. Finally, the cells were evaluated for viability.

HSE Preparation and TUNEL Assay. HSEs were produced from HaCaT cultures and human fibroblasts. Briefly, human fibroblasts were added to collagen I gel to maintain vitality and to proliferate the fibroblasts in the dermal-like component. Human keratinocytes have been plated on this substrate and subcultured for 7 days to allow the formation of the basal layers of the epidermis. They were subsequently subcultivated for 7 days under emergence conditions to allow the generation of the stratum corneum of the epidermis. Tissue sections of HSE were treated with UV-A under previously reported conditions, and the sample was analyzed for the presence of apoptotic cells using an *in situ* terminal deoxynucleotidyl transferase dUTP nick-end labeling (TUNEL-FITC) assay (Roche Applied Science) following the standard protocol. Cell nuclei were counterstained with DAPI solution (Thermo Fisher) and imaged using fluorescence microscopy.

■ ASSOCIATED CONTENT

Supporting Information

The Supporting Information is available free of charge at https://pubs.acs.org/doi/10.1021/acsomega.1c02268.

Figure S1, ^{31}P NMR characterization of starting lignin from a commercial source; and quantitative ^{31}P NMR spectra and signal assignment of each kind of lignin (PDF)

■ AUTHOR INFORMATION

Corresponding Author

Raffaele Saladino − *Department of Biological and Ecological Sciences, University of Tuscia, 01100 Viterbo, Italy;* orcid.org/0000-0002-4420-9063; Email: saladino@unitus.it

Authors

Davide Piccinino − *Department of Biological and Ecological Sciences, University of Tuscia, 01100 Viterbo, Italy*

Eliana Capecchi − *Department of Biological and Ecological Sciences, University of Tuscia, 01100 Viterbo, Italy*

Ines Delfino − *Department of Biological and Ecological Sciences, University of Tuscia, 01100 Viterbo, Italy*

Marcello Crucianelli − *Department of Physical and Chemical Sciences, University of Aquila, Coppito 67100 L'Aquila, Italy*

Nicola Conte − *IDI Farmaceutici, Pomezia 00071 Rome, Italy*

Daniele Avitabile − *IDI Farmaceutici, Pomezia 00071 Rome, Italy*

Complete contact information is available at: https://pubs.acs.org/10.1021/acsomega.1c02268

Author Contributions

All authors contributed equally to this work.

Notes

The authors declare no competing financial interest.

■ ACKNOWLEDGMENTS

The authors acknowledge the EU project-EASME/EMFF/Blue Economy-2018/n.863697 "FISH chitinolytic biowastes FOR FISH active and sustainable packaging material" (FISH4FISH)" and the FISR project LIOO "Laboratory of innovation of the olive-oil supply chain."

■ REFERENCES

(1) Ragauskas, A. J.; Beckham, G. T.; Biddy, M. J.; Chandra, R.; Chen, F.; Davis, M. F.; Davison, B. H.; Dixon, R. A.; Gilna, P.; Keller, M.; et al. Lignin valorization: Improving lignin processing in the biorefinery. *Science* **2014**, *344*, No. 124683.

(2) Ge, Y.; Li, Z. Application of Lignin and Its Derivatives in Adsorption of Heavy Metal Ions in Water: A Review. *ACS Sustainable Chem. Eng.* **2018**, *6*, 7181−7192.

(3) Dai, P.; Liang, M.; Ma, X.; Luo, Y.; He, M.; Gu, X.; Gu, Q.; Hussain, I.; Luo, Z. Highly Efficient, Environmentally Friendly Lignin-Based Flame Retardant Used in Epoxy Resin. *ACS Omega* **2020**, *5*, 32084−32093.

(4) Calvo-Flores, F. G.; Dobado, J. A. Lignin as renewable raw material. *ChemSusChem* **2010**, *3*, 1227−1235.

(5) Becker, J.; Wittmann, C. A field of dreams: Lignin valorization into chemicals, materials, fuels, and health-care products. *Biotechnol. Adv.* **2019**, *37*, No. 107360.

(6) Gil-Chávez, G. J.; Padhi, S. S. P.; Pereira, C. V.; Guerreiro, J. N.; Matias, A. A.; Smirnova, I. Cytotoxicity and biological capacity of sulfur-free lignins obtained in novel biorefining process. *Int. J. Biol. Macromol.* **2019**, *136*, 697−703.

(7) Figueiredo, P.; Lintinen, K.; Hirvonen, J. T.; Kostiainen, M. A.; Santos, H. A. Properties and chemical modifications of lignin: Towards lignin-based nanomaterials for biomedical applications. *Prog. Mater. Sci.* **2018**, *93*, 233−269.

(8) Dong, X.; Dong, M.; Lu, Y.; Turley, A.; Jin, T.; Wu, C. Antimicrobial and antioxidant activities of lignin from residue of corn stover to ethanol production. *Ind. Crops Prod.* **2011**, *34*, 1629−1634.

(9) Piccinino, D.; Capecchi, E.; Tomaino, E.; Gabellone, S.; Gigli, V.; Avitabile, D.; Saladino, R. Nano-Structured Lignin as Green Antioxidant and UV Shielding Ingredient for Sunscreen Applications. *Antioxidants* **2021**, *10*, No. 274.

(10) Kienberger, M.; Maitz, S.; Pichler, T.; Demmelmayer, P. Systematic Review on Isolation Processes for Technical Lignin. *Processes* **2021**, *9*, No. 804.

(11) Xiong, K.; Jin, C.; Liu, G. F.; Wu, G. M.; Chen, J.; Kong, Z. W. Preparation and characterization of lignin nanoparticles with controllable size by nanoprecipitation method. *Chem. Ind. For. Prod.* **2015**, *35*, 85−92.

(12) Piccinino, D.; Capecchi, E.; Botta, L.; Bizzarri, B. M.; Bollella, P.; Antiochia, R.; Saladino, R. Layer-by-Layer Preparation of Microcapsules and Nanocapsules of Mixed Polyphenols with High Antioxidant and UV-Shielding Properties. *Biomacromolecules* **2018**, *19*, 3883−3893.

(13) Figueiredo, P.; Lintinen, K.; Kiriazis, A.; Hynninen, V.; Liu, Z.; Bauleth-Ramos, T.; Rahikkala, A.; Correia, A.; Kohoutg, T.; Sarmento, B.; et al. In vitro evaluation of biodegradable lignin-based nanoparticles for drug delivery and enhanced antiproliferation effect in cancer cells. *Biomaterials* **2017**, *121*, 97−108.

(14) Botta, L.; Brunori, F.; Tulimieri, A.; Piccinino, D.; Meschini, R.; Saladino, R. Laccase-Mediated Enhancement of the Antioxidant Activity of Propolis and Poplar Bud Exudates. *ACS Omega* **2017**, *2*, 2515−2523.

(15) Piccinino, D.; Capecchi, E.; Botta, L.; Bollella, P.; Antiochia, R.; Crucianelli, M.; Saladino, R. Layer by layer supported laccase on

lignin nanoparticles catalyzes the selective oxidation of alcohols to aldehydes. *Catal. Sci. Technol.* **2019**, *9*, 4125−4134.
(16) Capecchi, E.; Piccinino, D.; Tomaino, E.; Bizzarri, B. M.; Polli, F.; Antiochia, R.; Mazzei, F.; Saladino, R. Lignin nanoparticles are renewable and functional platforms for the concanavalin a oriented immobilization of glucose oxidase−peroxidase in cascade bio-sensing. *RSC Adv.* **2020**, *10*, 29031−29042.
(17) Capecchi, E.; Piccinino, D.; Bizzarri, B. M.; Avitabile, D.; Pelosi, C.; Colantonio, C.; Calabrò, G.; Saladino, R. Enzyme-Lignin Nanocapsules Are Sustainable Catalysts and Vehicles for the Preparation of Unique Polyvalent Bioinks. *Biomacromolecules* **2019**, *20*, 1975−1988.
(18) Widsten, P.; Tamminen, T.; Liitiä, T. Natural Sunscreens Based on Nanoparticles of Modified Kraft Lignin (CatLignin). *ACS Omega* **2020**, *5*, 13438−13446.
(19) Lee, S. C.; Yoo, E.; Lee, S. H.; Won, K. Preparation and application of light-colored lignin nanoparticles for broad-spectrum sunscreens. *Polymers (Basel)* **2020**, *12*, No. 699.
(20) Manfredini, S.; Ziosi, P.; Vertuani, S.; Bustacchini, S. A reflex technology to improve sun filter by SPF booster effect. *J. Plast. Dermatology* **2009**, *5*, 37−40.
(21) Mishra, P. K.; Ekielski, A. The Self-Assembly of Lignin and Its Application in Nanoparticle Synthesis: A Short Review. *Nanomaterials* **2019**, *9*, No. 243.
(22) Wang, J.; Qian, Y.; Li, L.; Qiu, X. Atomic Force Microscopy and Molecular Dynamics Simulations for Study of Lignin Solution Self-Assembly Mechanisms in Organic−Aqueous Solvent Mixtures. *ChemSusChem* **2020**, *13*, 4420−4427.
(23) Leskinen, T.; Smyth, M.; Xiao, Y.; Lintinen, K.; Mattinen, M.-L.; Kostiainen, M. A.; Oinas, P.; Österberget, M. Scaling Up Production of Colloidal Lignin Particles. *Nord. Pulp Pap. Res. J.* **2017**, *32*, No. 586.
(24) Li, H.; Deng, Y.; Wu, H.; Ren, Y.; Qiu, X.; Zheng, D.; Li, C. Dafeng Zheng and ChunLi L. Self-assembly of kraft lignin into nanospheres in dioxane-water mixtures. *Holzforschung* **2016**, *70*, 725−731.
(25) Yearla, S. R.; Padmasree, K. Preparation and characterisation of lignin nanoparticles: Evaluation of their potential as antioxidants and UV protectants. *J. Exp. Nanosci.* **2016**, *11*, 289−302.
(26) Mishra, P. K.; Ekielski, A. A Simple Method to Synthesize Lignin Nanoparticles. *Colloids Interfaces* **2019**, *3*, No. 52.
(27) Zhu, J. Y.; Agarwal, U. P.; Ciesielski, P. N.; Himmel, M. E.; Gao, R.; Deng, Y.; Morits, M.; Österberg, M. Towards sustainable production and utilization of plant-biomass-based nanomaterials: A review and analysis of recent developments. *Biotechnol. Biofuels* **2021**, *14*, No. 114.
(28) Matsakas, L.; Karnaouri, A.; Cwirzen, A.; Rova, U.; Christakopoulos, P. Formation of lignin nanoparticles by combining organosolv pretreatment of birch biomass and homogenization processes. *Molecules* **2018**, *23*, No. 1822.
(29) Chen, L.; Shi, Y.; Gao, B.; Zhao, Y.; Jiang, Y.; Zha, Z.; Xue, W.; Gong, L. Lignin Nanoparticles: Green Synthesis in a γ-Valerolactone/Water Binary Solvent and Application to Enhance Antimicrobial Activity of Essential Oils. *ACS Sustainable Chem. Eng.* **2020**, *8*, 714−722.
(30) Bian, H.; Chen, L.; Gleisner, R.; Daia, H.; Zhu, J. Y. Producing wood-based nanomaterials by rapid fractionation of wood at 80 °C using a recyclable acid hydrotrope. *Green Chem.* **2017**, *19*, No. 3370.
(31) Luo, T.; Wang, C.; Ji, X.; Yang, G.; Chen, J.; Janaswamy, S.; Lyu, G. Preparation and Characterization of Size-Controlled Lignin Nanoparticles with Deep Eutectic Solvents by Nanoprecipitation. *Molecules* **2021**, *26*, No. 218.
(32) Machado, T. O.; Beckers, S. J.; Fischer, J.; Müller, B.; Sayer, C.; De Araújo, P. H. H.; Landfester, K.; Wurm, F. R. Bio-Based Lignin Nanocarriers Loaded with Fungicides as a Versatile Platform for Drug Delivery in Plants. *Biomacromolecules* **2020**, *21*, 2755−2763.
(33) Souza, V. G. L.; Fernando, L. A. Nanoparticles in food packaging: Biodegradability and potential migration to food−A review. *Food Packag. Shelf Life* **2016**, *8*, 63−70.
(34) Stiefel, C.; Schwack, W. Photoprotection in changing times−UV filter efficacy and safety, sensitization processes and regulatory aspects. *Int. J. Cosmet. Sci.* **2015**, *37*, 2−30.
(35) For a general overview in the topic see: a) www.cosmos-standard.org b) Corrêa, I.; Faria, R. P. V.; Rodrigues, A. E. Continuous Valorization of Glycerol into Solketal: Recent Advances on Catalysts, Processes, and Industrial Perspectives. *Sustain. Chem.* **2021**, *2*, 286−324.
(36) Zhang, H.; Grinstaff, M. W. Recent advances in glycerol polymers: Chemistry and biomedical applications. *Macromol. Rapid Commun.* **2014**, *35*, 1906−1924.
(37) Fowles, J. R.; Banton, M. I.; Pottenger, L. H. A toxicological review of the propylene glycols. *Crit. Rev. Toxicol.* **2013**, *43*, 363−390.
(38) Metz, D. J.; Glines, A. Density, viscosity, and dielectric constant of tetrahydrofuran between -78° and 30°C. *J. Phys. Chem.* **1967**, *71*, No. 1158.
(39) Zia, H.; Ma, J. K. H.; O'Donnell, J. P.; Luzzi, L. A. Cosolvency of Dimethyl Isosorbide for Steroid Solubility. *Pharm. Res.* **1991**, *8*, 502−504.
(40) Ismalaj, E.; Strappaveccia, G.; Ballerini, E.; Elisei, F.; Piermatti, O.; Gelman, D.; Vaccaro, L. γ-valerolactone as a renewable dipolar aprotic solvent deriving from biomass degradation for the Hiyama reaction. *ACS Sustainable Chem. Eng.* **2014**, *2*, 2461−2464.
(41) Ma, Q.; Chen, L.; Wang, R.; Yang, R.; Zhu, J. Y. Direct production of lignin nanoparticles (LNPs) from wood using p-toluenesulfonic acid in an aqueous system at 80°C: Characterization of LNP morphology, size, and surface charge. *Holzforschung* **2018**, *72*, 933−942.
(42) Sameni, J.; Krigstin, S.; Sain, M. Solubility of lignin and acetylated lignin in organic solvents,". *BioRes.* **2017**, *12*, 1548−1565.
(43) Bao, D.; Xie, Y.; Ma, S.; Wu, Z.; Piao, J. G. Self-assembly of a renewable lignin biopolymer in nanoparticles with multiple morphologies. *J. Appl. Polym. Sci.* **2019**, *136*, No. 47482.
(44) Qian, Y.; Deng, Y.; Qiu, X.; Li, H.; Yang, D. Formation of uniform colloidal spheres from lignin, a renewable resource recovered from pulping spent liquor. *Green Chem.* **2014**, *16*, 2156−2163.
(45) Rao, X.; Liu, Y.; Zhang, Q.; Chen, W.; Liu, Y.; Yu, H. Assembly of Organosolv Lignin Residues into Submicron Spheres: The Effects of Granulating in Ethanol/Water Mixtures and Homogenization. *ACS Omega* **2017**, *2*, 2858−2865.
(46) Xiong, F.; Han, Y.; Wang, S.; Li, G.; Qin, T.; Chen, Y.; Chu, F. Preparation and formation mechanism of size-controlled lignin nanospheres by self-assembly. *Ind. Crops Prod.* **2017**, *100*, 146−152.
(47) Silmore, K. S.; Gupta, C.; Washburn, N. R. Tunable Pickering emulsions with polymer-grafted lignin nanoparticles (PGLNs). *J. Colloid Interface Sci.* **2016**, *466*, 91−100.
(48) Tian, D.; Hu, J.; Chandra, R. P.; Saddler, J. N.; Lu, C. Valorizing Recalcitrant Cellulolytic Enzyme Lignin via Lignin Nanoparticles Fabrication in an Integrated Biorefinery. *ACS Sustainable Chem. Eng.* **2017**, *5*, 2702−2710.
(49) Zhao, W.; Xiao, L.-P.; Song, G.; Sun, R.-C.; He, L.; Singh, S.; Simmons, B. A.; Cheng, G. From lignin subunits to aggregates: Insights into lignin solubilization. *Green Chem.* **2017**, *19*, 3272−3281.
(50) Ju, T.; Zhang, Z.; Li, Y.; Miaoa, X.; Ji, J. Continuous production of lignin nanoparticles using a microchannel reactor and its application in UV-shielding films. *RSC Adv.* **2019**, *9*, 24915−24921.
(51) Qian, Y.; Qiu, X.; Zhu, S. Sunscreen performance of lignin from different technical resources and their general synergistic effect with synthetic sunscreens. *ACS Sustainable Chem. Eng.* **2016**, *4*, 4029−4035.
(52) Guerranti, C.; Martellini, T.; Perra, G.; Scopetani, C.; Cincinelli, A. Microplastics in cosmetics: Environmental issues and needs for global bans. *Environ. Toxicol. Pharmacol.* **2019**, *68*, 75−79.
(53) Vinardell, M. P.; Mitjans, M. Lignins and their derivatives with beneficial effects on human health. *Int. J. Mol. Sci.* **2017**, *18*, No. 1219.
(54) Zhang, Z.; Michniak-Kohn, B. B. Tissue engineered human skin equivalents. *Pharmaceutics* **2012**, *4*, 26−41.

https://doi.org/10.1021/acsomega.1c02268
ACS Omega 2021, 6, 21444−21456

(55) Huang, Y.; Law, J. C. F.; Lam, T. K.; Leung, K. S. Y. Risks of organic UV filters: A review of environmental and human health concern studies. *Sci. Total Environ.* **2021**, *755*, No. 142486.
(56) Nash, J. F.; Tanner, P. R. Relevance of UV filter/sunscreen product photostability to human safety. *Photodermatol., Photoimmunol. Photomed.* **2014**, *30*, 88−95.
(57) Korkina, L.; Kostyuk, V.; Potapovich, A.; Mayer, W.; Talib, N.; De Luca, C. Secondary plant metabolites for sun protective cosmetics: From pre-selection to product formulation. *Cosmetics* **2018**, *5*, No. 32.
(58) He, T.; Tsui, M. M. P.; Tan, C. J.; Ma, C. Y.; Yiu, S. K. F.; Wang, L. H.; Chen, T. H.; Fan, T. Y.; Lam, P. K. S.; Murphy, M. B. Toxicological effects of two organic ultraviolet filters and a related commercial sunscreen product in adult corals. *Environ. Pollut.* **2019**, *245*, 462−471.
(59) Matts, P. J.; Alard, V.; Brown, M. W.; Ferrero, L.; Gers-Barlag, H.; Issachar, N.; Moyal, D.; Wolber, R. The COLIPA in vitro UVA method: A standard and reproducible measure of sunscreen UVA protection. *Int. J. Cosmet. Sci.* **2010**, *32*, 35−46.

https://doi.org/10.1021/acsomega.1c02268
ACS Omega 2021, 6, 21444−21456